THE JOURNAL OF BIOLOGICAL CHEMISTRY VOL. 285, NO. 30, pp. 22936–22941, July 23, 2010
© 2010 by The American Society for Biochemistry and Molecular Biology, Inc. Printed in the U.S.A.

Identification of Tubulin Deglutamylase among *Caenorhabditis elegans* and Mammalian Cytosolic Carboxypeptidases (CCPs)*[S]◆

Received for publication, April 9, 2010, and in revised form, May 31, 2010 Published, JBC Papers in Press, June 2, 2010, DOI 10.1074/jbc.C110.128280

Yoshishige Kimura[‡], Nobuya Kurabe[‡], Koji Ikegami[‡], Koji Tsutsumi[‡], Yoshiyuki Konishi[‡], Oktay Ismail Kaplan[§], Hirofumi Kunitomo[¶], Yuichi Iino[¶], Oliver E. Blacque[§], and Mitsutoshi Setou[‡1]

From the [‡]Department of Molecular Anatomy, Hamamatsu University School of Medicine, 1-20-1 Handayama, Hamamatsu, Shizuoka 431-3192, Japan, the [§]School of Biomolecular and Biomedical Science, UCD Conway Institute, University College Dublin, Belfield, Dublin 4, Ireland, and the [¶]Department of Biophysics and Biochemistry, Graduate School of Science, the University of Tokyo, Tokyo 113-0032, Japan

Tubulin polyglutamylation is a reversible post-translational modification, serving important roles in microtubule (MT)-related processes. Polyglutamylases of the tubulin tyrosine ligase-like (TTLL) family add glutamate moieties to specific tubulin glutamate residues, whereas as yet unknown deglutamylases shorten polyglutamate chains. First we investigated regulatory machinery of tubulin glutamylation in MT-based sensory cilia of the roundworm *Caenorhabditis elegans*. We found that ciliary MTs were polyglutamylated by a process requiring *ttll-4*. Conversely, loss of *ccpp-6* gene function, which encodes one of two cytosolic carboxypeptidases (CCPs), resulted in elevated levels of ciliary MT polyglutamylation. Consistent with a deglutamylase function for *ccpp-6*, overexpression of this gene in ciliated cells decreased polyglutamylation signals. Similarly, we confirmed that overexpression of murine CCP5, one of two sequence orthologs of nematode *ccpp-6*, caused a dramatic loss of MT polyglutamylation in cultured mammalian cells. Finally, using an *in vitro* assay for tubulin glutamylation, we found that recombinantly expressed Myc-tagged CCP5 exhibited deglutamylase biochemical activities. Together, these data from two evolutionarily divergent systems identify *C. elegans* CCPP-6 and its mammalian ortholog CCP5 as a tubulin deglutamylase.

The microtubule (MT)[2] cytoskeleton plays critical roles in multiple cellular processes such as chromosome segregation, intracellular transport, cell morphogenesis, and polarity. Tubulin, which is the major protein subunit of MT fibers, exhibits polymorphic protein variation and undergoes a variety of unique post-translational modifications at its C-terminal tail, such as detyrosination/tyrosination (1, 2), polyglycylation (3), and polyglutamylation (4). These modifications regulate tubulin and MT function. Polyglutamylation enzymes add multiple glutamate moieties to specific glutamate residues within substrate proteins. Physiological roles of tubulin polyglutamylation for MT-related processes were reported recently (5, 6) and reviewed by Ikegami and Setou (7).

Polyglutamylase enzymes have recently been identified as belonging to the tubulin tyrosine ligase-like (TTLL) protein family (8–10) (supplemental Fig. 1). In contrast, the enzyme(s) underlying deglutamylation have not been discovered yet, although such proteins are suggested to be present in mouse brain neurons and in cultured cells (11, 12).

In this study, we employed the genetically tractable nematode, *Caenorhabditis elegans*, to identify genes that regulate tubulin polyglutamylation/deglutamylation. Specifically, we investigated tubulin post-translational modification in *C. elegans* sensory cilia, which are MT-based organelles that extend from the distal dendrite tips of 60 sensory neurons found in sensory organs named amphid (head) and phasmid (tail) sensilla (see Fig. 1*A*). In this system, we identified a cytosolic carboxypeptidase (*ccpp*) gene, *ccpp-6*, as a candidate tubulin deglutamylase gene, whose functional properties are opposite to those of the tubulin polyglutamylase gene, *ttll-4*. Furthermore, we identified mammalian CCP5 as a functional homolog of nematode CCPP-6 and confirmed its deglutamylase activity in cultured cells and *in vitro*. To our knowledge, this is the first report revealing the molecular nature of the tubulin deglutamylase enzyme.

EXPERIMENTAL PROCEDURES

Worm Culture and Genetics—Nematodes were grown and maintained at 20 °C under standard conditions (13). All mutant and transgenic strains used in this study are listed in the supplemental Methods.

Immunohistochemical Analyses—Immunohistochemical analyses were performed as described in previous studies (14) with a slight modification. Full details are described in the supplemental Methods.

C. elegans Microscopy and Image Analysis—Immunostained worm samples were mounted on a slide glass with VECTASHIELD (Vector Laboratories) and analyzed under an FV1000 confocal microscope (Olympus). At least 20 adult worms for each strain were analyzed, and all images were collected using

* This work was supported by a SENTAN grant from the Japan Science and Technology Agency and WAKATE grants from the Japan Society for the Promotion of Science (Grant WAKATE S to M. S. and Grant WAKATE B to Y. Konishi).

◆ This article was selected as a Paper of the Week.

[S] The on-line version of this article (available at http://www.jbc.org) contains supplemental methods and references, Figs. 1–10, Table 1, and Movie 1.

[1] To whom correspondence should be addressed. Tel./Fax: 81-53-435-2292; E-mail: setou@hama-med.ac.jp.

[2] The abbreviations used are: MT, microtubule; TTLL, tubulin tyrosine ligase-like; CCP, cytosolic carboxypeptidase; CCPP, cytosolic carboxypeptidase (*C. elegans*); mAb, monoclonal antibody; GFP, green fluorescent protein; RNAi, RNA interference; PIPES, 1,4-piperazinediethanesulfonic acid.

the same optical condition. Images were analyzed using FV10-ASW software (Olympus). Immunostained polyglutamylated (GT335) and α-tubulin signal intensities were measured in sensory cilia from the same optical slice. Following subtraction of background signals in non-ciliary regions, a GT335/α-tubulin signal intensity ratio was calculated for each image. GT335/α-tubulin ratios were averaged for each strain. The relative intensity of each strain was obtained from the average of GT335/α-tubulin normalized by that of wild type and statistically analyzed by StatPlus (AnalystSoft).

Cell Culture and RNAi—The conventional methods of cell culture and gene knockdown by RNAi are described in the supplemental Methods.

In Vitro Deglutamylase Assay—Expression plasmids for CCP5 or -6 fused to a Myc tag (pCMV-tag3a-CCP5 and pCMV-tag3c-CCP6) were introduced into HEK293T cells using Lipofectamine 2000 (Invitrogen). Cells were lysed with PIPES-based buffer. For immunoprecipitation, the lysates were incubated with anti-Myc polyclonal antibody (Bethyl Laboratories) and subsequently precipitated with protein G-Sepharose beads (GE Healthcare). Tubulin deglutamylation assays were performed by adding 1.25 μg of porcine tubulin either to cell lysates or to immunoprecipitated Myc-CCP5 at 25 °C. Reactions were terminated by diluting mixtures with 2× SDS-PAGE sample buffer at 15 min. Samples were then subjected to Western blotting using GT335 (1:5000), anti-α-tubulin polyclonal (1:5000), and anti-Myc 9E10 (1:1000) antibodies.

RESULTS AND DISCUSSION

C. elegans Sensory Ciliary MTs Are Strongly Polyglutamylated, Requiring ttll-4—We determined the distribution of polyglutamylation signals in *C. elegans* sensory cilia using antibodies that specifically recognize polyglutamylation. Using the monoclonal antibody (mAb) GT335, which specifically recognizes both monoglutamylation and polyglutamylation (10), robust signals were detected in the ciliary regions of the nematode head and tail (Fig. 1, *A* and *B*, *left*; supplemental Fig. 2*A*; and supplemental Movie 1). To ensure that the observed signals are indeed those of ciliary MTs, we employed strains expressing ciliated cell-specific transcriptional GFP transgenes (derived from promoter-GFP constructs), which illuminate the entire sensory neuron. In such strains, we found that the cilia of most amphid head neurons (ASE, ADF, ASH, ASK, AWA, AWC, and AFD) showed GT335 signals (Fig. 1*B* *middle* and *right*; supplemental Fig. 3). Strong signals were also seen in the ciliary structures of the inner (Fig. 1*B*, *left panel*, *white arrows*) and outer labial sensilla (Fig. 1*B*, *left panel*, *yellow arrows*; supplemental Movie 1). In contrast, no GT335 signals were detected in other ciliary neurons such as the neurons of the cephalic sensilla (supplemental Fig. 3, *bottom row*, *arrow*). In the tail, the ciliary structures of the phasmid neurons PHA, PHB, and PQR were also labeled with GT335 (supplemental Fig. 2*B*). Another mAb, B3, which specifically recognizes polyglutamylated tubulins (15), yielded similar signal staining patterns (supplemental Fig. 2*C*). Together, these data show that the MTs of *C. elegans* sensory cilia are highly polyglutamylated.

Tubulin polyglutamylation is mediated by enzymes of the TTLL family (8–10). The *C. elegans* genome contains six TTLL genes (*ttll-4*, *-5*, *-9*, *-11*, *-12*, and *-15*), and each gene belongs to a different clade (supplemental Fig. 1). Next, we studied the expression pattern of *C. elegans ttll* genes using transgenic worms carrying transcriptional GFP reporters (GFP directed by *ttll* promoter) or translational GFP reporters (GFP was fused to the entire open reading frame of the gene) under the control of the endogenous promoter of the gene (supplemental Figs. 4 and 5; summarized in supplemental Table 1). We found that three *ttll* genes, *ttll-4*, *-9*, and *-11*, are expressed in many ciliated sensory neurons in amphid (supplemental Fig. 5, *D* and *F–H*). *C. elegans* does not have any polyglycylase orthologs (TTLL3, -8, and -10) (16–18), which are found in other animals having motile cilia (18, 19), where polyglycylation exclusively occurs. Consistent with an absence of motile cilia and polyglycylase orthologs in *C. elegans*, immunostaining for polyglycylation in worms revealed no signals.[3]

To identify which *ttll* gene contributes to the polyglutamylation observed in the sensory cilia, we studied worm strains with mutations in the *ttll* genes (summarized in supplemental Table 1). The GT335 signals completely disappeared in *ttll-4* worms (Fig. 1*C*, *second row*, *asterisks*, and *D*). To clearly evaluate the level of tubulin polyglutamylation, we quantified the signals of GT335 and of counterstained α-tubulin (Fig. 1*C*, *middle column*). The complete loss of GT335 signal was greater than a partial decrease of the α-tubulin signal in *ttll-4* mutants (Fig. 1*D*). In contrast, only a slight reduction in GT335 signals was observed (Fig. 1, *C*, *third row*, and *D*, $p < 0.01$, Student's *t* test). We observed no overt decrease of GT335 immunoreactivities in a hypomorphic *ttll-11*(*gk482*) mutant (data not shown). The GT335 immunoreactivities were not altered in *ttll-5(tm3360)* and *ttll-15(tm3871)* mutants (data not shown), presumably because these genes are not expressed in ciliated sensory neurons (supplemental Fig. 5, *E* and *J*). The prominent loss of polyglutamylation observed in the *ttll-4* mutant was reversed by overexpression of *ttll-4*::mCherry in sensory neurons (Fig. 1, *C bottom row*, and *D*). These findings demonstrate that TTLL-4 is a key enzyme that autonomously mediates tubulin polyglutamylation in sensory cilia.

CCPP-6 Is a Tubulin Deglutamylase in C. elegans—Previous reports suggest the presence of dynamic reversible regulation of tubulin polyglutamylation by deglutamylase activity (11, 12). Having identified TTLL-4 as a critical protein for tubulin polyglutamylation in *C. elegans* sensory cilia, we next turned our attention to identifying candidate deglutamylase genes in *C. elegans*. Cytosolic carboxypeptidases (CCPs) were recently identified as a subfamily of M14 metallocarboxypeptidases (20, 21). CCP1/Nna1, the first identified member of the CCP family, is mutated in Purkinje cell degeneration (*pcd*) mice (22); in these mice, the mitral cells in olfactory bulb show decreased signals of detyrosinated tubulins (20). *C. elegans* has only two CCP genes in its genome, F56H1.5 and EEED8.6, which we name here *ccpp-1* and *-6*, respectively by their amino acid similarity and protein structure in comparison with six mammalian CCP genes (*CCP1–6*) (Fig. 2*A*; supplemental Fig. 6). CCPP-1 belongs to the

[3] Y. Kimura and M. Setou, unpublished data.

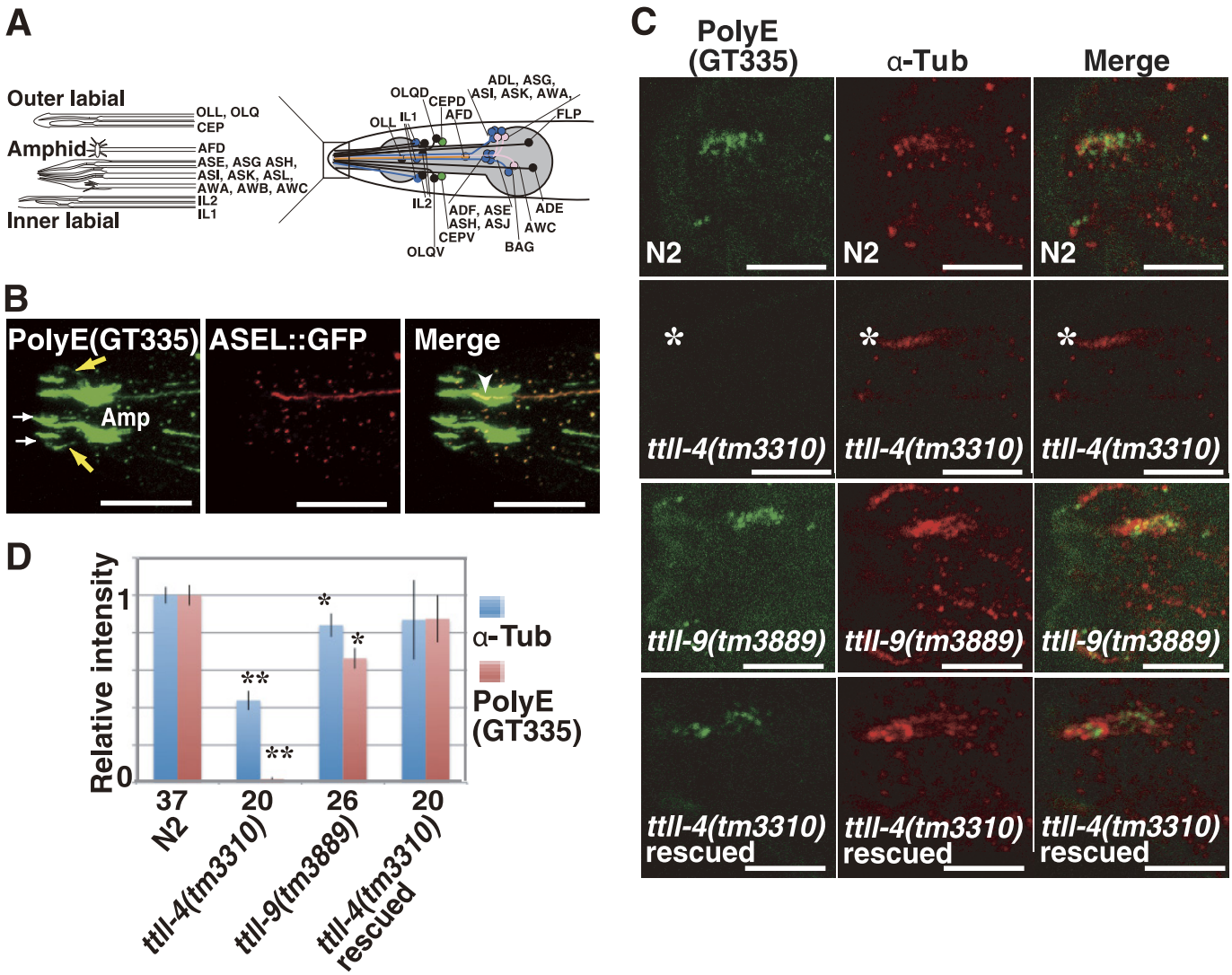

FIGURE 1. ***C. elegans* sensory cilia are abundant in tubulin polyglutamylation, which depends on *ttll-4*.** *A*, schematic diagram of a worm head that illustrates the positions of the ciliated cell bodies (*right*) and their ending (*left*). *B*, results of immunohistochemical analysis of head (around tip of nose) using GT335, which recognizes polyglutamylated tubulins. Signals can be observed in the amphids (*Amp*), inner labial (*arrows*), and outer labial neurons (*yellow arrows*). Worms that express GFP in the ASEL neuron were double-stained with GT335 (*left panel*) and anti-GFP polyclonal antibody (*middle panel*). Tubulin polyglutamylation signal is co-localized with ASEL marker, *gcy-7*::GFP (*right panel*, *arrowhead*). *PolyE*, polyglutamylation signal recognized by GT335. *C*, results of immunohistochemical analyses of *ttll* mutants by using GT335 (*left column*) together with a polyclonal antibody against α-tubulin (*α-Tub*, *middle column*), and merged (*right column*) under highly stringent conditions to detect GT335 signals more sensitively (see the supplemental Methods), which made GT335 signals a dotted pattern. *N2*, wild type; *ttll-4*(*tm3310*), *ttll-4* mutant; *ttll-9*(*tm3889*), *ttll-9* mutant; *ttll-4*(*tm3310*) *rescued*, *ttll-4* mutant rescued by the expression of TTLL-4::mCherry. *D*, quantified results of immunoreactivity analyses for α-tubulin (*blue bars*) and GT335 relative to α-tubulin (*red bars*). *Asterisks* ($p < 0.01$, Student's *t* test) and *double asterisks* ($p < 0.001$, Student's *t* test) indicate significant difference as compared with the wild type. Numbers of animals scored are indicated. *Bars* indicate mean ± S.E. All *scale bars* = 5 μm.

M14D3 group with mammalian CCP1 and -4, and CCPP-6 belongs to the M14D2 group with mammalian CCP5 and -6 (Fig. 2*A*).

To determine whether *ccpp-1* and *-6* are involved in the regulation of tubulin polyglutamylation, we first examined their expression in sensory neurons. A transcriptional GFP reporter of *ccpp-1* was expressed in amphid neurons (supplemental Fig. 7*C*). On the other hand, that of *ccpp-6* was expressed only in the labial neurons but not in amphid neurons (data not shown).

A translational reporter mCherry fused to CCPP-1 protein showed the weak dotted signals around the pharynx (supplemental Fig. 7*D*, *arrowheads*). Meanwhile, a translational GFP reporter for *ccpp-6* showed weak signals in the cell body of putative amphid neurons (supplemental Fig. 7, *A* and *B*, *arrowheads*), suggesting that expression in amphid cells was regulated by an enhancer element in a *ccpp-6* intron(s). The weak signals observed for GFP/mCherry-tagged CCPP-1 and CCPP-6 transgenes indicate that both CCPP proteins are maintained at very low levels, possibly because they are rapidly degraded. Nevertheless, these results suggest that both CCPP-1 and CCPP-6 are expressed and function cell autonomously in amphid neurons.

Importantly, we found a robust reduction in the GT335 signals in the cilia of CCPP-6::GFP-expressing animals ($p < 0.001$, Student's *t* test), consistent with our hypothesis that CCPP-6 functions as a deglutamylase (Fig. 2, *B*, *third row*, *asterisks*, and *D*, *upper panel*). In contrast, the GT335 signals did not decrease in the CCPP-1::mCherry-expressing animals. Rather,

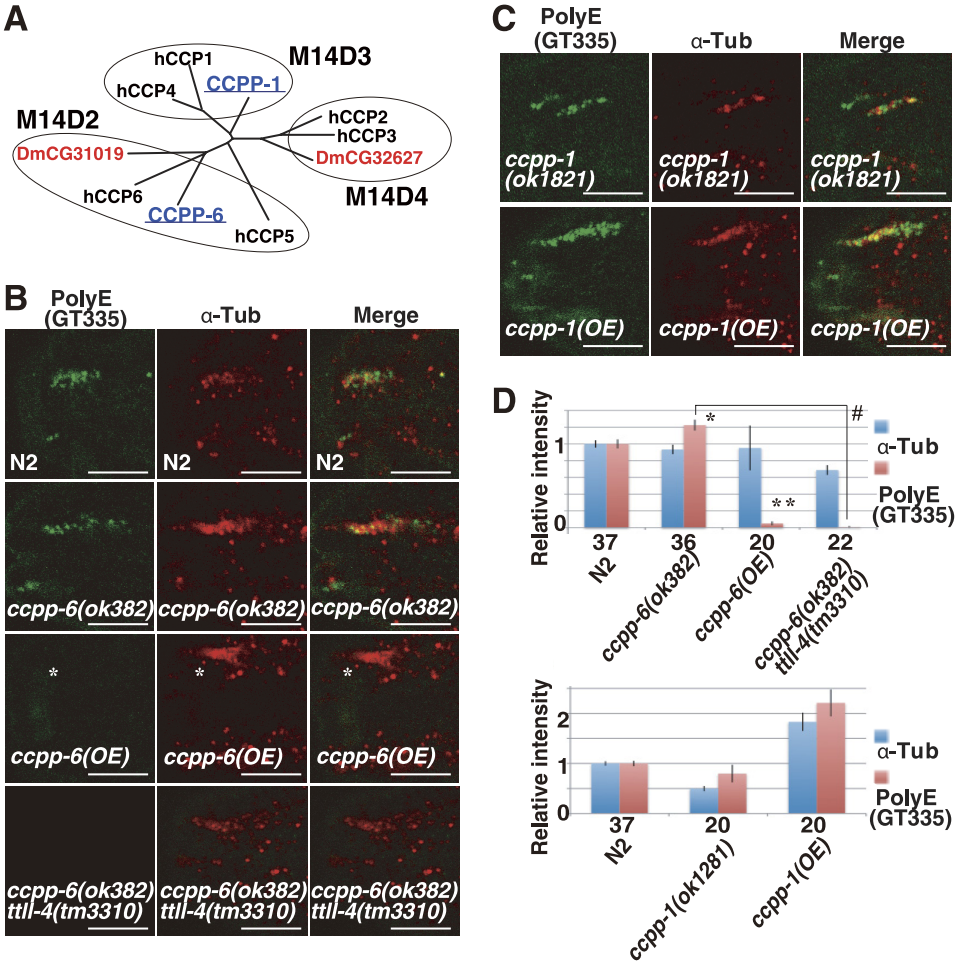

FIGURE 2. **The cytosolic CCP gene *ccpp-6* suppresses tubulin polyglutamylation.** *A*, phylogenic tree of CCP proteins among *Homo sapiens*, *Drosophila melanogaster*, and *C. elegans*. This tree was calculated and drawn in comparison with CP domains by the ClustalW alignment program. Predicted proteins of *C. elegans*, *H. sapiens*, and *D. melanogaster* are colored *blue*, *black*, and *red*, respectively. *Circles* surrounding the genes indicate the clades of this gene family (M14D2–3). *B*, results of the immunohistochemical analysis of *ccpp-6* mutant performed as shown in Fig. 1. Signals of GT335 and α-tubulin (*α-Tub*) detected in each strain are shown as follows: wild type (*N2*), *ccpp-6*(*ok382*), and *ccpp-6*(*OE*), in which *ccpp-6* is overexpressed by CCPP-6::mCherry and the *ttll-4(tm3310); ccpp-6(ok382)* double mutant. *PolyE*, polyglutamylation signal recognized by GT335. *C*, results of the immunohistochemical analysis of *ccpp-1*(*ok1281*) and *ccpp-1*(*OE*) in which *ccpp-1* is overexpressed by CCPP-1::GFP. *D*, measurement of the results for *ccpp-6* (*upper*) and *ccpp-1* (*lower*). *Asterisks* ($p < 0.05$, Student's *t* test) and *double asterisks* ($p < 0.001$, Student's *t* test) indicate significant difference as compared with the wild type. *Number sign* indicates significant decrease ($p < 0.001$) of the *ccpp-6*(*ok382*);*ttll-4*(*tm3310*) double mutant to the *ccpp-6*(*ok382*) single mutant. Numbers of animals scored are indicated. *Bars* indicate mean ± S.E. All *scale bars* = 5 μm.

the amphids of these animals showed increased GT335 signals along with the increase in the tubulin signals (Fig. 2, *C*, *lower row*, and *D*, *lower panel*). Hence, CCPP-1 might be involved in regulating tubulin function in the sensory cilia but does not likely act as a deglutamylase.

To determine whether endogenous CCPP-6 negatively regulates tubulin polyglutamylation, we analyzed tubulin polyglutamylation in *ccpp-6* mutants. The tubulin GT335 signal significantly increased in *ccpp-6* mutants ($p < 0.05$, Student's *t* test), indicating that CCPP-6 suppresses tubulin polyglutamylation (Fig. 2, *B*, *second row*, and *D*, *upper panel*). This enhanced signal is completely lost in the *ccpp-6*;*ttll-4* double mutant background (Fig. 2, *B*, *bottom row*, and *D*, *upper panel*). These results indicate that *ccpp-6* negatively regulates tubulin polyglutamylation in sensory cilia; this suggests that CCPP-6 is a tubulin deglutamylase.

Mammalian CCP5 Functions as a Tubulin Deglutamylase—We next examined whether mammalian CCPs (Fig. 2*A*) harbor tubulin deglutamylase(s). To this end, we exogenously overexpressed Myc-tagged CCP5 and -6, which are orthologs of *C. elegans* CCPP-6, and CCP2 as a control along with tubulin polyglutamylases, TTLL5 and -6, in HEK293T cells. Remarkably, GT335-detected tubulin bands completely disappeared when CCP5 was expressed (Fig. 3*A*). We could not detect such an effect for CCP2 and -6 at least in our system (Fig. 3*A*, data not shown). Strikingly, CCP5 did show no effect on the level of tyrosinated tubulin (Fig. 3*B*), indicating that CCP5 does not have detyrosinase activity. This deglutamylation activity was also detected for other proteins (supplemental Fig. 8, *arrowheads*). We further analyzed the effect of CCP5 in the endogenous polyglutamylation by the overexpression in mouse cortical neurons. The CCP5-expressing cells showed marked reduction in the GT335 signals (Fig. 3*C*, *middle column*).

To further examine whether mammalian CCP5 effectively counteracts tubulin polyglutamylation, we performed RNAi treatment of CCP5 in NIH3T3 cells. Two independent small interfering RNAs against CCP5 clearly increased intensities of GT335-detected bands at 50 kDa (Fig. 3*D*), which was overlapped with the β-tubulin band (Fig. 3*D*; *green versus red*). The two-dimensional electrophoresis revealed that the CCP5 knockdown caused an increase in the intensity of GT335-detected β-tubulin spots (Fig. 3*E*, *top row*), and more acidic β-tubulin spots were detected (Fig. 3*E*, *bottom row*). These results indicate that CCP5, one of the sequence orthologs of nematode CCPP-6 (Fig. 2*A*), is a tubulin deglutamylase in mammalian cells. The reason why β-tubulin polyglutamylation is effectively increased in CCP5 knockdown cells could be explained by the presence of endogenous glutamylation activity preferential to β-tubulin in non-neuronal cells (12).

We next carried out an *in vitro* enzyme assay of recombinant CCP5. We first tried to use nematode CCPP-6 and murine CCP5 expressed in bacteria. However, these recombinants did not show the enzyme activity or were hardly solubilized (see the supplemental Methods). This is probably because CCPP-6 and CCP5 fails to fold into the correct three-dimensional

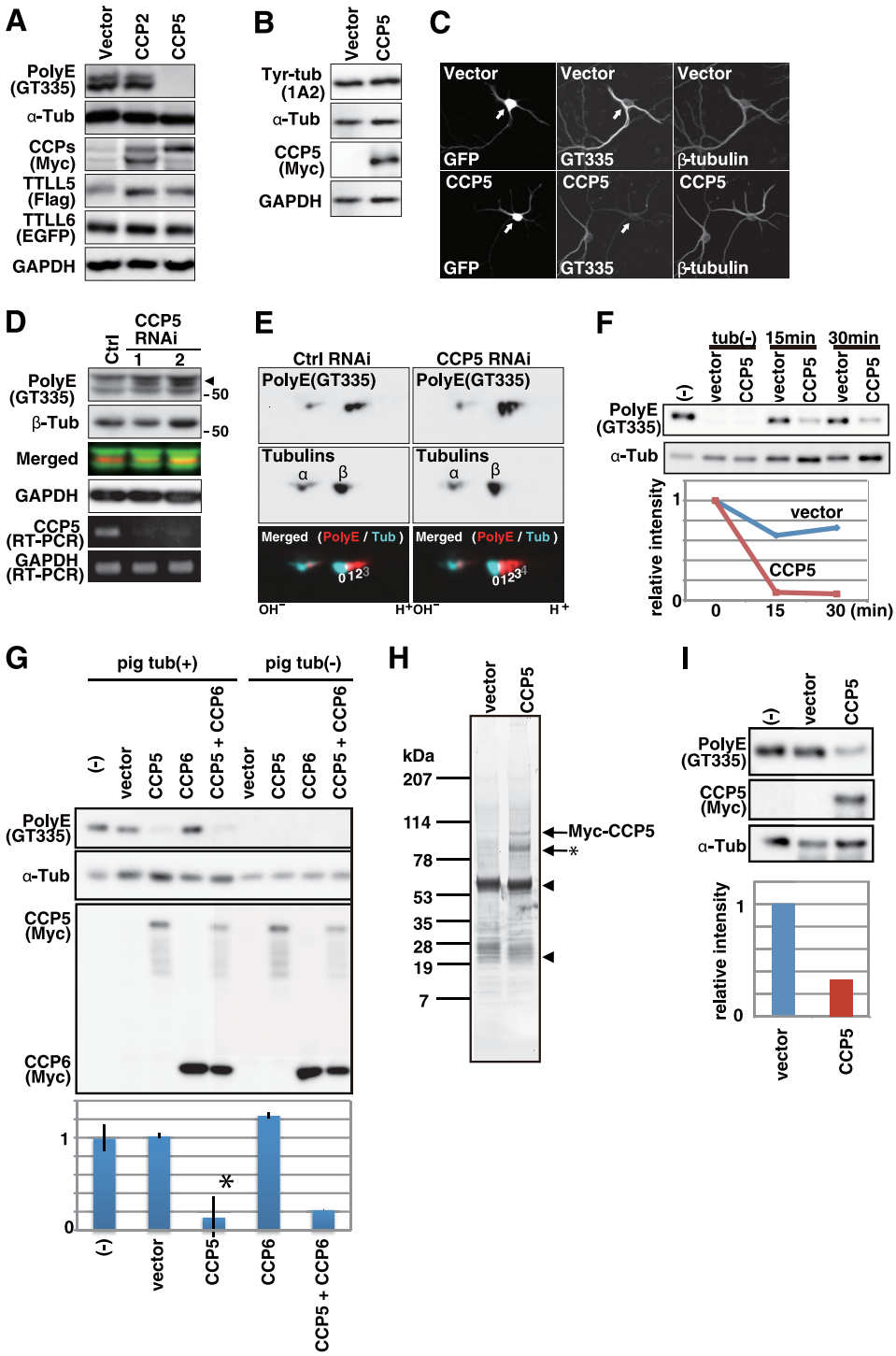

FIGURE 3. **Murine CCP5 has tubulin deglutamylase activity.** *A*, murine CCP2 or -5 was expressed in HEK293T cells along with TTLL5 and -6. *PolyE*, polyglutamylation signal recognized by GT335; *α-Tub*, α-tubulin; *EGFP*, enhanced GFP; *GAPDH*, glyceraldehyde-3-phosphate dehydrogenase. *B*, murine CCP5 alone was expressed in HEK293T cells. *C*, cortical neurons (6 days *in vitro*) in which a vector for GFP together with the expression plasmid for CCP5 or its control vector was introduced were subjected to the immunocytochemistry by using GT335 and β-tubulin antibody. *D*, two independent stealth small interfering RNAs were introduced into NIH-3T3 cells. CCP5 knockdown samples were subjected to the long range SDS-PAGE and reverse transcription-PCR. The *arrowhead* points to the newly emerging band, which is overlapped with the β-tubulin band. *E*, two-dimensional electrophoresis of CCP5 knockdown cell lysates. The numbers of predicted glutamates added to β-tubulin represent are numerically indicated. *F*, *in vitro* enzyme assay was performed by using pig tubulin as a substrate and CCP5-expressing HEK293T lysate as the enzyme source. Reaction mixture was analyzed by Western blotting with GT335. *G*, comparison between CCP5 and -6 enzyme activity *in vitro*. *In vitro* enzyme assay was performed in the same optimized condition as in *F*. CCP5-expressing lysate showed significant reduction (*, $p < 0.05$), whereas CCP6-expressing lysate did not show activity in this condition. The reaction with a mixture of both lysates did not show any enhancement. *Bars* indicate mean ± S.E. *H*, CCP5-expressing and control HEK293T cell lysates were immunoprecipitated with anti-Myc polyclonal antibody. The immunoprecipitants were electrophoresed using 5–20% gradient gel and stained with SYPRO Ruby protein stain. Protein bands indicated by an *asterisk* were the putative degradation products of Myc-CCP5 (supplemental Fig. 10). The *arrowheads* indicate subunits of immunoglobulin. *I*, after immunoprecipitation, immunoprecipitants were analyzed by *in vitro* enzyme assay using pig tubulin as a substrate. Measurement results were indicated in the *bottom chart*. The lanes with (−) in *E*, *G*, and *I* indicate the substrate pig tubulin without lysate treatment.

structure when expressed in bacteria. Thus, we decided to use Myc-tagged CCP5 expressed in HEK293T cells and successfully detected deglutamylase activity *in vitro* (Fig. 3, *F* and *G*; supplemental Fig. 9). The salt concentration drastically affected the CCP5 activity in the cell lysates; the enzyme was more active with 100 mM NaCl than with 0 or 50 mM NaCl (supplemental Fig. 9). CCP5 activity appeared to be saturated at 15 min as the decrease in GT335 signals of tubulin reached plateau (Fig. 3*F*). The faint decrease of GT335 signals in the mock transfection sample could be caused by the presence of endogenous deglutamylase in the cell lysates as reported previously (11, 12). The increase of α-tubulin signals in CCP5-containing samples could occur by the preferential binding of anti-α-tubulin antibody to less glutamylated tubulins (6, 23).

Despite the highest similarity between nematode CCPP-6 and mammalian CCP6, we were not able to detect deglutamylase activity of CCP6 in cultured cells. We were not able to detect the reduction of GT335 signal in the *in vitro* assay either (Fig. 3*G*). We would not, however, exclude possibilities that CCP6 functions as a deglutamylase. CCP6 might function under other experimental conditions or act on specific substrates, *e.g.* axonemal tubulins in cilia, as CCPP-6 works in the sensory cilia of *C. elegans*.

Finally, we challenged the enzyme activity assay by using Myc-CCP5 immobilized on antibody-protein G beads. In the immunoprecipitant of anti-Myc antibody, the antibody-purified CCP5 was detected in a major band (Fig. 3*H*). The broad bands with the faster migration than Myc-CCP5 (Fig. 3*H*, *asterisk*) were likely to be degraded Myc-CCP5 as the anti-Myc antibody detected some proteins at the same position (supplemental Fig. 10). Other minor bands seemed to be nonspecifically precipitated proteins because they were also detected in the bead fraction of the empty vector-transfected cell lysates. Thus, Myc-CCP5 was the major and specific component of the immunoprecipitant. Incubation of substrate pig brain tubulin with this immobilized Myc-CCP5 showed clear reduction in the GT335 signal (Fig. 3*I*). The background activity detected in cell lysates (Fig. 3*F*) was completely eliminated in this assay (Fig. 3*I*). Taken together, these results clearly demonstrate that CCP5 has a tubulin deglutamylase activity.

Conclusion—By the genetic approach with *C. elegans*, we isolated CCPP-6 as a negative regulator of tubulin polyglutamylation *in vivo*. We also demonstrated that CCP5, a mammalian sequence ortholog of CCPP-6, had clear enzyme activity of tubulin deglutamylase by *in vitro* assay. In conclusion, we have identified *C. elegans* CCPP-6 and mammalian CCP5 as a tubulin deglutamylase by both *in vitro* and *in vivo* assay results.

Acknowledgments—We thank Dr. N. Hisamoto and Dr. K. Matsumoto for helpful discussions; Dr. C. Janke for providing the mAb GT335; Dr. S. Mitani and the C. elegans Genetics Center for providing the mutant strains; Dr. Y. Kohara for providing the cDNAs; and Dr. A. Fire and Dr. J. Culotti for providing the plasmids.

REFERENCES

1. Argaraña, C. E., Barra, H. S., and Caputto, R. (1978) *Mol. Cell Biochem.* **19,** 17–21
2. Gundersen, G. G., Kalnoski, M. H., and Bulinski, J. C. (1984) *Cell* **38,** 779–789
3. Redeker, V., Levilliers, N., Schmitter, J. M., Le Caer, J. P., Rossier, J., Adoutte, A., and Bré, M. H. (1994) *Science* **266,** 1688–1691
4. Eddé, B., Rossier, J., Le Caer, J. P., Desbruyères, E., Gros, F., and Denoulet, P. (1990) *Science* **247,** 83–85
5. Ikegami, K., Sato, S., Nakamura, K., Ostrowski, L. E., and Setou, M. (2010) *Proc. Natl. Acad. Sci. U.S.A.* **107,** 10490–10495
6. Ikegami, K., Heier, R. L., Taruishi, M., Takagi, H., Mukai, M., Shimma, S., Taira, S., Hatanaka, K., Morone, N., Yao, I., Campbell, P. K., Yuasa, S., Janke, C., Macgregor, G. R., and Setou, M. (2007) *Proc. Natl. Acad. Sci. U.S.A.* **104,** 3213–3218
7. Ikegami, K., and Setou, M. (2010) *Cell Struct. Funct.* **35,** 15–22
8. Ikegami, K., Mukai, M., Tsuchida, J., Heier, R. L., Macgregor, G. R., and Setou, M. (2006) *J. Biol. Chem.* **281,** 30707–30716
9. Janke, C., Rogowski, K., Wloga, D., Regnard, C., Kajava, A. V., Strub, J. M., Temurak, N., van Dijk, J., Boucher, D., van Dorsselaer, A., Suryavanshi, S., Gaertig, J., and Eddé, B. (2005) *Science* **308,** 1758–1762
10. van Dijk, J., Rogowski, K., Miro, J., Lacroix, B., Eddé, B., and Janke, C. (2007) *Mol. Cell* **26,** 437–448
11. Audebert, S., Desbruyères, E., Gruszczynski, C., Koulakoff, A., Gros, F., Denoulet, P., and Eddé, B. (1993) *Mol. Biol. Cell* **4,** 615–626
12. Regnard, C., Desbruyères, E., Denoulet, P., and Eddé, B. (1999) *J. Cell Sci.* **112,** 4281–4289
13. Brenner, S. (1974) *Genetics* **77,** 71–94
14. Nonet, M. L., Staunton, J. E., Kilgard, M. P., Fergestad, T., Hartwieg, E., Horvitz, H. R., Jorgensen, E. M., and Meyer, B. J. (1997) *J. Neurosci.* **17,** 8061–8073
15. Gagnon, C., White, D., Cosson, J., Huitorel, P., Eddé, B., Desbruyères, E., Paturle-Lafanechère, L., Multigner, L., Job, D., and Cibert, C. (1996) *J. Cell Sci.* **109,** 1545–1553
16. Ikegami, K., Horigome, D., Mukai, M., Livnat, I., MacGregor, G. R., and Setou, M. (2008) *FEBS Lett.* **582,** 1129–1134
17. Ikegami, K., and Setou, M. (2009) *FEBS Lett.* **583,** 1957–1963
18. Rogowski, K., Juge, F., van Dijk, J., Wloga, D., Strub, J. M., Levilliers, N., Thomas, D., Bré, M. H., Van Dorsselaer, A., Gaertig, J., and Janke, C. (2009) *Cell* **137,** 1076–1087
19. Wloga, D., Webster, D. M., Rogowski, K., Bré, M. H., Levilliers, N., Jerka-Dziadosz, M., Janke, C., Dougan, S. T., and Gaertig, J. (2009) *Dev. Cell* **16,** 867–876
20. Kalinina, E., Biswas, R., Berezniuk, I., Hermoso, A., Aviles, F. X., and Fricker, L. D. (2007) *FASEB J.* **21,** 836–850
21. Rodriguez de la Vega, M., Sevilla, R. G., Hermoso, A., Lorenzo, J., Tanco, S., Diez, A., Fricker, L. D., Bautista, J. M., and Avilés, F. X. (2007) *FASEB J.* **21,** 851–865
22. Fernandez-Gonzalez, A., La Spada, A. R., Treadaway, J., Higdon, J. C., Harris, B. S., Sidman, R. L., Morgan, J. I., and Zuo, J. (2002) *Science* **295,** 1904–1906
23. Bré, M. H., de Néchaud, B., Wolff, A., and Fleury, A. (1994) *Cell Motil. Cytoskeleton* **27,** 337–349